Available online at www.sciencedirect.com
ScienceDirect
Journal of the European Ceramic Society 27 (2007) 3385–3390
www.elsevier.com/locate/jeurceramsoc

Symbiosis between grain boundary sliding and slip creep to obtain high-strain-rate superplasticity in aluminum alloys

Jorge A. del Valle, M. Teresa Pérez-Prado, Oscar A. Ruano *

Department of Physical Metallurgy, Centro Nacional de Investigaciones Metalúrgicas, CSIC, Av. Gregorio del Amo 8, 28040 Madrid, Spain

Available online 17 April 2007

Abstract

Aluminum alloys with a fine and recrystallized microstructure deform by grain boundary sliding at low strain rates. However, some aluminum alloys, for instance, Al–5% Ca–5% Zn, Supral 2004, Al–Li 2090, Al–Li 8090, show indications of slip creep and grain boundary sliding at a given temperature and strain rate inside the superplastic range. These materials, in addition, deform superplastically even at high-strain rates (10^{-2} to 10^{-1} s^{-1}). The simultaneous operation of grain boundary sliding (GBS) and slip creep is a surprising observation since these two deformation mechanisms usually act independently of one another. The one yielding the highest strain rate becomes rate controlling and thus the main contributor to the total strain. In this paper, microstructure (including microtexture) as well as mechanical property data of several Al alloys are reviewed with the aim of seeking further understanding on the symbiosis between GBS and slip creep.

Keywords: Superplasticity; Mechanical properties; Creep

1. Introduction

It is well established that grain boundary sliding (GBS), at low strain rates, and creep by glide plus climb also named slip creep, at high-strain rates, are the controlling mechanisms that operate during high temperature deformation of fine-grained metallic materials.[1–3] These two deformation mechanisms, being independent from one another, act simultaneously, and in general the fastest controls creep in a given strain rate or stress range.

Fine-grained materials deforming by grain boundary sliding possess an enhanced ductility, or superplasticity. Initial equiaxed grains remain equiaxed in spite of the large elongations achieved and usually significant texture weakening takes place due to multiple random grain rotations.[2]

Several aluminum alloys are capable of undergoing significant tensile extension before failure when tested at rather high-strain rates[4–8] (10^{-2} to 10^{-1} s^{-1}). This anomalous behavior has been attributed to the operation of both crystallographic slip (CS) and GBS in response to the applied stress over a wide range of strain rates, which violates well-accepted models predicting the rate controlling deformation mechanisms at high temperature. In this investigation extensive data on the microstructural evolution of a number of high-strain-rate superplastic aluminum alloys, as well as on their mechanical behavior, is compiled. It deals with the deformation properties of fine-grained aluminum alloys that exhibit superplasticity mainly at elevated temperatures (327–527 °C (600–800 K), i.e., 0.7–0.85T_m) and under high and medium strain rates. These data are compared with data from other aluminum alloys that have shown superplasticity at medium strain rates. The behavior of all these aluminum alloys are analyzed on the light of the interaction between grain boundary sliding and slip creep and the influence of microstructure gradients along the sheet thickness.

2. Deformation behavior of superplastic aluminum alloys

2.1. Aluminum alloys with fine equiaxed grains before deformation

Fig. 1 shows creep data for a set of aluminum alloys where conventional superplastic behavior is present. Most of the data were obtained by means of strain-rate-change tests in a constant displacement machine. The creep rate, normalized by the lattice diffusion and the grain size is represented as a function of the modulus normalized stress. The reference of the investigations[4,11–22] is given in Table 1. The line given in the

* Corresponding author. Tel.: +34 915538900; fax: +34 915347425.
E-mail address: ruano@cenim.csic.es (O.A. Ruano).

0955-2219/$ – see front matter © 2007 Elsevier Ltd. All rights reserved.
doi:10.1016/j.jeurceramsoc.2007.02.185

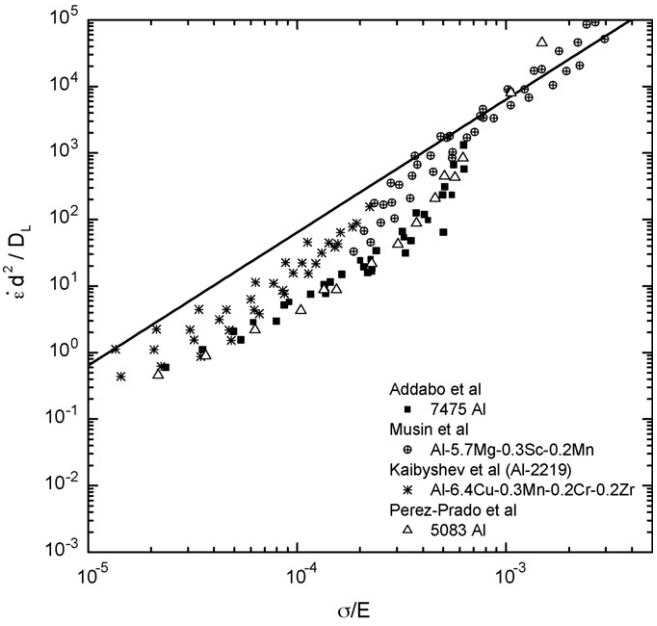

Fig. 1. Diffusion and grain size normalized strain rate as a function of modulus normalized stress for various aluminum alloys with fine equiaxed grains before deformation.

figure corresponds to the prediction of the phenomenological relation for grain boundary sliding controlled by lattice self-diffusion[1]:

$$\dot{\varepsilon} = A\frac{D_L}{d^2}\left(\frac{\sigma}{E}\right)^2 \quad (1)$$

where E is the unrelaxed average polycrystalline Young's modulus of aluminum, A is a constant, d is the grain size and D_L is the lattice diffusion coefficient ($D_L = 1.7 \times 10^{-4}$ (m^2/s) exp ($-Q/RT$), where $Q = 142$ kJ/mol). The value of constant A in this equation has been obtained by fitting all type of superplastic materials[1], and not only Al alloys, and it is 6.4×10^9 s^{-1}. The creep equation fits the data rather well although the average value of the pre-exponential constant is about a factor of 5 lower than that given in the equation. It is worth noting that the normalized strain rate of Fig. 1 corresponds to the GBS region. The figure includes also data from the slip creep region that has no grain size dependence. Therefore, these data should not be taken into account. In addition, it should be noted that the data of Musin et al., that correspond to an ultrafine grain material has the highest value of A. This will be discussed in a future publication. All the aluminum alloys given in the figure were static annealed before the test. This produced fine equiaxed grains by discontinuous recrystallization. The texture usually had a random or weak cube component and almost disappeared after deformation. Large elongations to failure are obtained in the superplastic regime and the stress exponent is about two. The grains remained equiaxed during the test and some grain growth was observed. This is explained by a GBS mechanism being the dominant mode of deformation. The only importance of slip creep in this regime is as an accommodation process for GBS which ensures grain compatibility. Dislocations close to the grain boundary are considered to be important to close the cavities at triple junctions preventing the operation of GBS. This explains the low stress exponent obtained according to various models[1], the most known of them is that from Ball and Hutchison.[9,10] This accommodation process is interdependent with GBS and the slower will be rate controlling. Finally, at high-strain rates, higher stress exponents and a reinforcement of specific texture components (usually the <1 1 1> fiber) are obtained. This is consistent with a slip creep mechanism, usually with $n = 5$, working independently of GBS since both mechanisms are independent of one another.

2.2. Aluminum alloys without a recrystallized microstructure before deformation

Fig. 2 shows creep data for a different set of aluminum alloys from those given in Fig. 1. The reference of the

Table 1
Reference data used to elaborate Figs. 1 and 2

Alloy	T (°C)	Grain size (μm)[a]	Reference
Al–6Cu–0.4Zr	440–520 (713–793 K)	13.2	[11]
Al–21Cu–0.4Zr	440–520 (713–793 K)	13.2	[11]
Al–34Cu–0.4Zr	440–520 (713–793 K)	13.2	[11]
Al–33Cu	400–450 (673–723 K)	13.7	[12]
Al–5Ca–5Zn	300–550 (573–823 K)	2	[4]
Al–7.6Ca	450–550 (723–823 K)	9	[13]
Al–9.3Zn–1Mg–0.2Zr	520 (793 K)	17.1	[14]
Al–6Mg–0.4Zr (Supral)	430–520 (703–793 K)	13.2	[15]
Al–5.6Zn–1.6Mg–0.4Zr	430–520 (703–793 K)	15.5	[16]
Al–10.7Zn–0.4Zr	450–550 (703–823 K)	12.2	[16]
Al–3Cu–2Li–1Mg–0.2Zr; Al–2.5Li–1.5Cu–1Mg–0.1Zr	400–500 (673–773 K)	2–3	[17]
Al–5.7Mg–0.32Sc	250–450 (523–723 K)	2.6–7.7[b]	[18]
Al–6.4Cu–0.3Mn–0.2Cr–0.2Zr	450–540 (723–813 K)	25.6–50.1[b]	[19]
Al–7475	400–515 (673–788 K)	20.9	[20]
Al 5083	335–435 (608–808 K)	22.1	[21]
Al–6Cu–0.4Zr	450 (723 K)	5	[22]

[a] Grain sizes were recalculated using $d = 1.74 \times$ average linear intercept length.
[b] The grain sizes vary depending on test temperature, the grain sizes were calculated using a transverse-longitudinal average × 1.74.

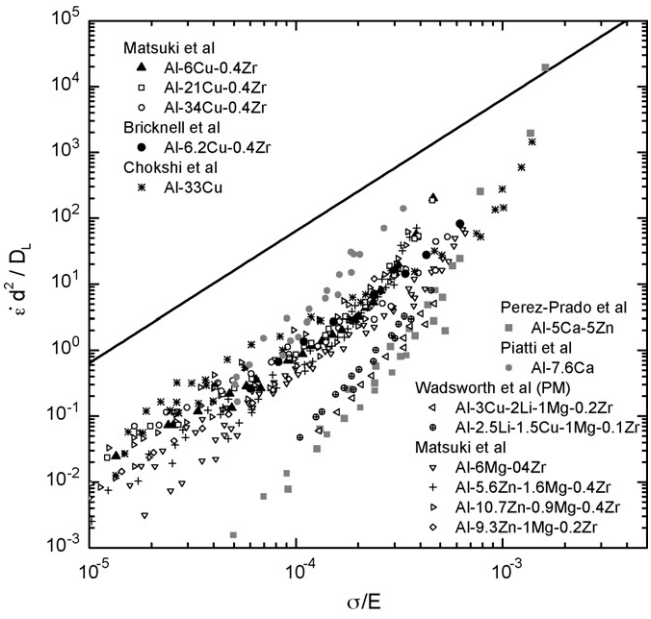

Fig. 2. Diffusion and grain size normalized strain rate as a function of modulus normalized stress for various aluminum alloys without a recrystallized microstructure before deformation.

investigations[4,11–22] is given in Table 1. These alloys are reported to show slip creep in the superplastic regime. The line given in the figure corresponds to the prediction of the phenomenological relation for grain boundary sliding controlled by lattice self-diffusion. The value of the pre-exponential constant of these alloys is much lower than the value given in the phenomenological equation, between 100 and 5000 times lower. The alloys given in the figure are not fully recrystallized at the beginning of the test in spite of a short annealing treatment. On the contrary, the final step of their thermomechanical processing usually involves a cold rolling step. Thus, the superplastic Al alloys given in the figure have usually a deformation-induced initial microstructure, formed by grains that are elongated along the rolling direction (RD) and subdivided into cells and cell blocks.[4,8] The materials have deformation textures such as the brass, copper and S texture. The textures of the as-received alloys are typical rolling textures, with the main components located within the α and β fibers in Euler space. Fig. 3(a) depicts the initial texture of the Al–5% Ca–5% Zn alloy, by means of the (1 1 1) pole figure.[5] The main component is a copper-type ori-

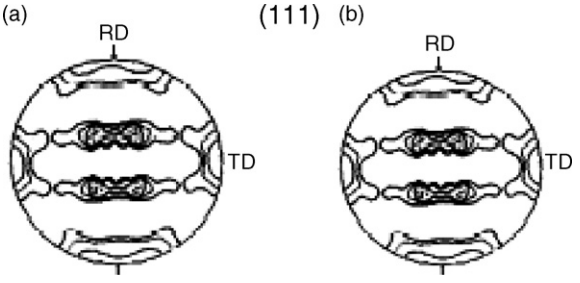

Fig. 3. (a) Texture of the as-received Al–5% Ca–5% Zn alloy; (b) texture of the as-received Al–5% Ca–5% Zn alloy deformed at 400 °C and 10^{-2} s^{-1} along the transverse direction.

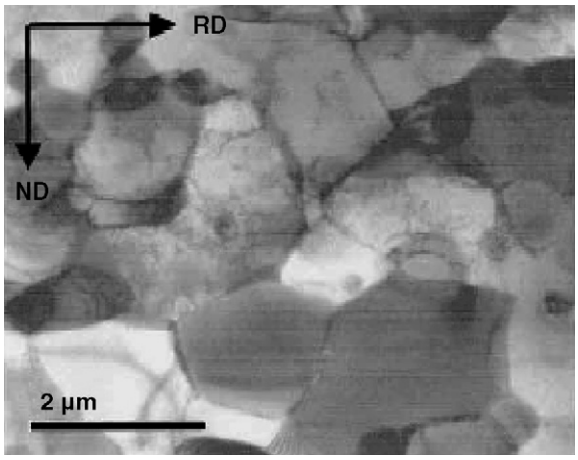

Fig. 4. Transmission electron microscopy micrograph showing the microstructure of the as-received Al–5% Ca–5% Zn alloy.

entation. Usually cold rolling reductions close or higher than 90% are used, giving rise to geometrical thinning of the grains down to thicknesses that are smaller than 1 μm. As an example, Fig. 4 illustrates the as-processed microstructure of the Al–5% Ca–5% Zn alloy.[4] Average cell size is about 500 nm. In addition, these alloys commonly contain a dispersion of fine second phase particles that impedes significant microstructural changes during static annealing.

However, with the concourse of deformation and temperature, as occurs during testing under superplastic conditions, this microstructure evolves gradually towards a fully recrystallized microstructure. At the very first stages of deformation, crystallographic slip is the main deformation mechanism since, in spite of the fine-scale of the structure, the number of high angle boundaries, capable of sliding, is relatively small. As deformation proceeds, different slip systems are activated in different areas within the elongated grains, leading to local rotations of the lattice toward various end orientations. Thus, grain subdivision by the formation of geometrically necessary boundaries (GNBs) ensues. During these first stages of deformation, significant texture changes take place. Shifts in the main components along the β fiber, toward the C component ({1 1 2}<1 1 1>) during longitudinal tests (tensile axis – TA – parallel to RD) and toward the B component ({0 1 1}<2 1 1>) during transverse tests (tensile axis – TA – perpendicular to RD) are observed. Texture weakening rarely occurs. Instead, well-defined texture components develop. As an example, Fig. 3(b) illustrates the texture of the as-received Al–5% Ca–5% Zn alloy deformed at 400 °C and 10^{-2} s^{-1} along the transverse direction. The main component is now a B orientation. This is consistent with well known models for lattice rotation upon deformation by slip in fcc materials.[23] Significant grain growth is not observed at the high-strain rates involved. Grain subdivision proceeds in this fashion until new high angle boundaries, readily able to slide, are created, i.e., in situ grain refinement takes place and a recrystallized structure develops. The amount of deformation needed to obtain this state is strongly dependent of the alloy composition and on the initial microstructure. The elimination of the initially deformed microstructure is thus achieved by a mechanism different from conventional

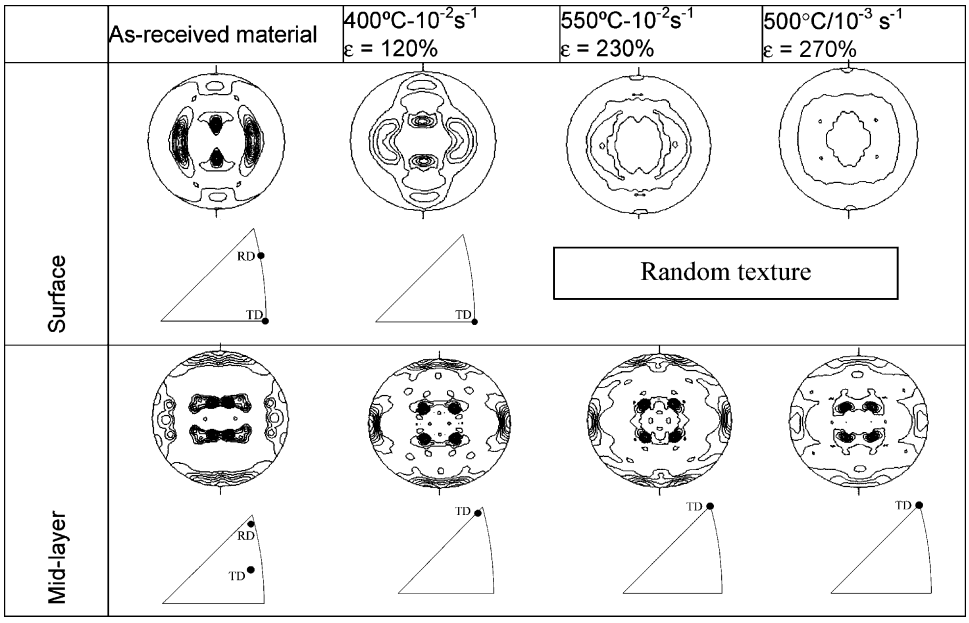

Fig. 5. (1 1 1) pole figures and inverse pole figure corresponding to the 8090 alloy in the as-received condition and after uniaxial deformation under different conditions of temperature and strain rate. In the direct pole figures, the rolling direction is the vertical direction and the transverse direction is the horizontal direction. Data corresponding to the surface and mid-layer areas are illustrated.

dynamic recrystallization since mainly slip processes and recovery are involved. This process has been assigned several names in the past decades, such as continuous dynamic recrystallization (CDRX),[4,24,25] and, lately, subdivision by GNB formation[26] (also in situ recrystallization and extended recovery[24]). Once a fully recrystallized structure is obtained, grain boundary sliding takes over slip creep as the main deformation mechanism. This causes the onset of texture weakening. Commonly failure takes place before complete randomization is achieved.

It is worth noting that a thermomechanical treatment of Supral to minimize the deformed microstructure at the beginning of deformation causes an increase of about one order of magnitude in the A value of the GBS equation respect to the alloy without the treatment.[27,28]

3. Microstructure and texture gradients

We have described in previous sections that superplastic alloys may be categorized into two different groups, attending to their initial microstructure. In some occasions both types of behavior coexist in the same material as a consequence of the microstructural and texture gradients.[6,7] In such cases the main texture components in the outer and mid-layers are located at different positions within the fibers. Texture gradients that are present in the initial microstructure may lead to premature facture by cavitation at the interfaces.[6]

A description of the microstructural and textural evolution of the as-received 8090 alloy sheet (Al–2.5% Li, 1.3% Cu, 0.9% Mg, 0.1% Zr) is presented in the following. The creep data of this alloy is similar to that reported by Wadsworth et al. included in Fig. 1 and Table 1. The ODF reveals that the main component in the outer layer (surface) is the {1 1 3}<3 3 2> orientation ($\varphi_1 = 90°$, $\Phi = 25°$, $\varphi_2 = 45°$) and in the mid-layer, the main texture component is the {1 5 6}<8 7 7> orientation ($\varphi_1 = 45°$, $\Phi = 50°$, $\varphi_2 = 10°$). The RD and TD directions are located along the [0 1 1]–[1 1 1] boundary of the stereographic triangle. Fig. 5 illustrates the (1 1 1) pole figures and inverse pole figures corresponding to the 8090 alloy in the as-received condition and after uniaxial deformation along the TD under different conditions of temperature and strain rate. Data corresponding to the surface and mid-layer areas are shown. The evolution of the texture upon deformation at high temperatures is very different in the surface and mid-layer areas. In the surface, texture randomization takes place readily. A significant decrease of the texture intensity can be already seen after deformation at 400 °C and 10^{-2} s^{-1}, where an elongation to fracture of 120% was attained. Uniaxial deformation at 550 °C and 10^{-2} s^{-1} (elongation to failure = 230%) results in a complete texture randomization. The decrease in the texture intensity during superplastic deformation is consistent with the operation of grain boundary sliding.

In the present case, the rapid loss of texture suggests that this mechanism predominates from the very first stages of deformation. The evolution of the texture in the mid-layer is, however, completely different. The texture intensity strengthens during deformation and significant lattice rotation (evidenced by the shift of the tensile axis, TD, along the [0 1 1]–[1 1 1] boundary of the stereographic triangle toward the [1 1 1] pole) takes place. These particular texture changes reveal the predominance of crystallographic slip as the main deformation mechanism.

The different rate of texture change in the surface and mid-layer of this 8090 alloy reveals the presence of a microstructural gradient. Grain boundary sliding takes place readily in the outer areas likely due to the presence of a large fraction of high angle boundaries. However, the mid-layer is probably a typical deformation structure, formed by grains elongated along the RD and a substructure of subgrains/cells, where only sluggish sliding

could take place. Thus, crystallographic slip is favored at the first stages of deformation, leading to lattice rotations.

It should be noticed that the highest elongation achieved in this alloy (270%) under optimum superplastic conditions of temperature and strain rate is only moderate when compared with other superplastic alloys. A possible explanation for this observation is the strain incompatibility at the interface between the outer and mid-layers. In fact, layer separation was observed after failure.

4. Discussion

Aluminum alloys that have fine equiaxed grains at the start of the test, as those given in Fig. 1, have a normal superplastic behavior. This means that almost from the start of the tests, GBS controls deformation and the texture is reduced progressively with strain. The *A* parameter of the GBS equation (Eq. (1)) has a relatively high value which reflects the easy of deformation of these alloys.

The changes of texture during deformation of the aluminum alloys given in Fig. 2 have led several authors to propose that slip plays an important role in the superplastic behavior of the alloys with an initial deformation microstructure,[29–32] i.e., slip acts as a primary deformation mechanism and not just as an accommodation process for grain boundary sliding. These authors state that the models of superplastic deformation based on grain boundary sliding or grain switching are not appropriate for describing the deformation behavior. A speculative model has been proposed recently by Bate et al.[32] based on strain rate-sensitive slip. Intragranular slip and viscous glide are considered at the origin of this high sensitivity. The role of grain boundary sliding is as an accommodation mechanism for slip. However, the authors mention that this model cannot predict the strain-rate sensitivities measured in Supral.

The incorporation of slip creep as the mechanism controlling deformation, and therefore the strain, and grain boundary sliding acting as an accommodation mechanism is ruled out from the standpoint of creep deformation mechanics: both mechanisms cannot control deformation simultaneously except in a short range of strain rates corresponding to a transition region from one to the other mechanism. Apart from this, the quite equiaxed shape of the grains, after extremely high elongations, remain to be explained.

Slip, however, has to be considered as an important contribution of deformation since the alloys given in Fig. 2 show strong dislocation activity and changes in texture as a function of deformation. An important factor that has to be considered during deformation is the contribution of CDRX or GNB formation. This type of recrystallization causes, basically, an increase in the misorientation angle between different regions within the grain with increasing deformation and has a strong influence on the deformation mechanisms involved. At the start of deformation, the alloy is not ready to sustain grain boundary sliding due to the heavily deformed microstructure present. The deformation, by slip, is quite stable since the strong work hardening observed in the alloys eliminates necking of the sample. This explains the rotation of the tensile axis towards the <1 1 1> direction in most of the grains which is the stable orientation in FCC materials. After some amount of deformation, fine equiaxed grains start to form as a consequence of the continuous recrystallization process. These new grains are able to rotate but are surrounded by elongated grains that deform by crystallographic slip. The fine grains after, say, 80% deformation are so numerous that the alloys can be considered to have a bimodal distribution of grain sizes. The fine grains may deform by a low stress exponent mechanism and the coarse grains may be subjected to slip creep.[33] The overall observed response of these materials would be a weighted sum of the two processes. In this exceptional situation, both deformation mechanisms may operate simultaneously. The symbiosis of these two mechanisms, that gives n values greater than 2, occurs for a transition strain rate larger than for conventional superplasticity since the dominance of high-strain exponent slip creep ($n=5$) is delayed. A consequence of this symbiosis is the attainment of high-strain-rate superplasticity. Indeed, although the elongation to failure of these alloys is usually lower than those deforming by conventional GBS (the alloys given in Fig. 1), low values of the stress exponent, and therefore high elongations, can be obtained at strain rates up to $10^{-1}\ s^{-1}$.

5. Conclusions

The high temperature deformation of various superplastic aluminum alloys has been reviewed. Aluminum alloys that have fine equiaxed grains at the start of the test deform mainly by GBS at low strain rates with only small evidence of dislocation activity. At high-strain rates, slip creep is the controlling mechanism. In contrast, during deformation of the alloys that have a deformation (generally rolling) microstructure at the start of the test, slip creep and continuous dynamic recrystallization (CDRX) have an important contribution since dislocation activity and changes in texture are observed during superplastic deformation. Therefore, slip creep predominates at small strains because the boundaries cannot sustain GBS. For an extended range of strain rates, new equiaxed grains, surrounded by high angle boundaries, are formed by CDRX inside the elongated grains. GBS takes place readily in those grains, leading to texture randomization. Low values of the constant *A* of the GBS equation are obtained which attests to the difficulty for deformation of these alloys. The symbiosis of GBS and slip creep allows having superplastic properties at high-strain rate. Texture gradients are often found in these alloys which influence the interpretation of the results because GBS and slip creep may be controlling deformation in different regions of the same tensile sample.

Acknowledgement

Thanks are given to CICYT for Grant MAT2003/1172.

References

[1]. Ruano, O. A. and Sherby, O. D., On constitutive equations for various diffusion-controlled creep mechanisms. *Rev. Phys. Appl.*, 1988, **23**, 625–637.

[2]. Nieh, T. G., Wadsworth, J. and Sherby, O. D., *Superplasticity in Metals and Ceramics*. Cambridge University Press, Cambridge, UK, 1997.
[3]. Kassner, M. E. and Pérez-Prado, M. T., Five power law creep in metals and alloys. *Prog. Mater. Sci.*, 2000, **45**, 1–102.
[4]. Pérez-Prado, M. T., McNelley, T. R., González-Doncel, G. and Ruano, O. A., Texture analysis of the transition from slip to grain boundary sliding in a continuously recrystallized superplastic aluminum alloy. *Mater. Sci. Eng.*, 2003, **A342**, 216–230.
[5]. Pérez-Prado, M. T., Cristina, M. C. and Ruano, O. A., Grain boundary and crystallographic slip during superplasticity of Al–5% Ca–5% Zn as studied by texture analysis. *Mater. Sci. Eng.*, 1998, **A244**, 216–223.
[6]. Pérez-Prado, M. T., Cristina, M. C., Ruano, O. A. and González-Doncel, G., Deformation mechanisms of superplastic Al–Li 8090 alloy examined by X-ray texture measurements. *Mater. Trans. JIM*, 2000, **41**, 1562–1568.
[7]. Pérez-Prado, M. T., Cristina, M. C., Ruano, O. A. and González-Doncel, G., Study of the deformation mechanisms of the superplastic Alloy Al–Li 2090 by texture analysis. *Textures Microstruct.*, 2000, **34**, 205–216.
[8]. McNelley, T. R., Swisher, D. L. and Pérez-Prado, M. T., Deformation bands and the formation of grain boundaries in a superplastic aluminum alloy. *Metall. Trans. A*, 2002, **33**, 279–290.
[9]. Ball, A. and Hutchison, M. M., Superplasticity in the Al–Zn eutectoid. *Mater. Sci. J.*, 1969, **3**, 1–7.
[10]. Ball, A., Superplasticity in the aluminium–zinc eutectoid—an early model revisited. *Mater. Sci. Eng.*, 1997, **A234**, 365–369.
[11]. Matsuki, K., Minami, K., Tokizawa, M. and Murakami, Y., Superplastic behaviour in nominally single-phase and two-phase Al–Cu alloys. *Met. Sci.*, 1979, **13**, 619–626.
[12]. Chokshi, A. H. and Langdon, T. G., The mechanical properties of the superplastic Al–33 Pct Cu eutectic alloy. *Metall. Trans.*, 1988, **19A**, 2487–2496.
[13]. Piatti, G., Pellegrini, G. and Trippodo, R., The tensile properties of a new superplastic aluminium alloy: Al–Al_4Ca eutectic. *J. Mater. Sci.*, 1976, **11**, 186–189.
[14]. Matsuki, K., Morita, H., Yamada, M. and Murakami, Y., Relative motion of grains during superplastic flow in an Al–9Zn–1 wt.% Mg alloy. *Met. Sci.*, 1977, **11**, 156–163.
[15]. Matsuki, K., Uetani, Y., Yamada, M. and Murakami, Y., Superplasticity in an Al–6 wt.% Mg alloy. *Met. Sci.*, 1976, **10**, 235–242.
[16]. Matsuki, K. and Yamada, M., Superplastic behavior of Al–Zn–Mg alloys. *J. Jpn. Inst. Met.*, 1973, **37**, 448–454.
[17]. Wadsworth, J. and Pelton, A. R., Superplastic behavior of a powder-source aluminium–lithium based alloy. *Scripta Metall.*, 1984, **18**, 387–392.
[18]. Musin, F., Kaibyshev, R., Motohashi, Y. and Itoh, G., High strain rate superplasticity in a commercial Al–Mg–Sc alloy. *Scripta Mater.*, 2004, **50**, 511–516.
[19]. Kaibyshev, R., Kazakulov, I., Gromov, D., Musin, F., Lesuer, D. R. and Nieh, T. G., Superplasticity in a 2219 aluminum alloy. *Scripta Mater.*, 2001, **44**, 2411–2417.
[20]. Adabbo, H. E., González-Doncel, G., Ruano, O. A., Belzunce, J. M. and Sherby, O. D., Strain hardening during superplastic deformation of Al-7475 alloy. *J. Mater. Res.*, 1989, **4**, 587–594.
[21]. Pérez-Prado, M. T., González-Doncel, G., Ruano, O. A. and McNelley, T. R., Texture analysis of the transition form slip to grain boundary sliding in a discontinuously recrystallized superplastic aluminum alloy. *Acta Mater.*, 2001, **49**, 2259–2268.
[22]. Bricknell, R. H. and Edington, J. W., Deformation characteristics of an Al–6Cu–0.4Zr superplastic alloy. *Metall. Trans.*, 1979, **10A**, 1257–1263.
[23]. Reid, C. N., *Deformation Geometry for Materials Scientists*. Pergamon Press, New York, 1973.
[24]. Humphreys, F. J. and Hatherly, M., *Recrystallization and Related Annealing Phenomena*. Pergamon Press, Oxford, UK, 1995.
[25]. Gourdet, S. and Montheillet, F., A model of continuous dynamic recrystallization. *Acta Mater.*, 2003, **51**, 2685–2699.
[26]. Kassner, M. E. and Barrabes, S. R., New developments in geometric dynamic recrystallization. *Mater. Sci. Eng.*, 2005, **A410–411**, 152–155.
[27]. Padmanabhan, K. A., Hirsch, J. and Lücke, K., Superplasticity-dislocation creep interactions in a coarse grained Al–Cu–Zr alloy. *J. Mater. Sci.*, 1991, **26**, 5309–5317.
[28]. Eddahbi, M., PhD Thesis, Universidad Complutense de Madrid, 1998.
[29]. Edington, J. W., Melton, K. N. and Cutler, C. P., Superplasticity. *Prog. Mater. Sci.*, 1976, **21**, 61–158.
[30]. Edington, J. W., Microstructural aspects of superplasticity. *Metall. Trans.*, 1982, **13A**, 703–715.
[31]. Blackwell, P. L. and Bate, P. S., The absence of relative grain translation during superplastic deformation of an Al–Li–Mg–Cu–Zr alloy. *Metall. Trans.*, 1993, **24A**, 1085–1093.
[32]. Bate, P. S., Humphreys, F. J., Ridley, N. and Zhang, B., Microstructure and texture evolution in the tension of superplastic Al–6Cu–0.4Zr. *Acta Mater.*, 2005, **53**, 3059–3069.
[33]. Ghosh, A. K. and Raj, R., Grain size distribution in superplasticity. *Acta Metall.*, 1981, **29**, 607–616.